

# Imaging molecular adsorbates: Resolution effects and determination of adsorption parameters

S. Chiang and V. M. Hallmark

*IBM Research Division, Almaden Research Center, San Jose, California 95120-6099*

K.-P. Meinhardt and K. Hafner

*Institut für Organische Chemie, Technische Hochschule Darmstadt, Darmstadt, Germany*

(Received 9 August 1993; accepted 23 December 1993)

The scanning tunneling microscope has been used to distinguish a series of related molecules (naphthalene, azulene, and various methylazulenes) on Pt(111) on the basis of their shape. Typical lower resolution images are used to measure the relative sticking coefficients and relative diffusion rates of the molecules. The orientations and binding sites of several of the molecules on the surface are also assigned. Tip dependent higher resolution images can show internal structural details on molecular species which have low diffusion rates.

## I. INTRODUCTION

The adsorption of small molecules on clean metal surfaces has been a field of study in surface science for many years because of its applications to catalysis, corrosion, and etching. In recent years, the development of the scanning tunneling microscope (STM) has enabled real-space imaging of individual molecules on surfaces,<sup>1</sup> leading to the hope that in the future complex molecular reactions may be observable. In particular, the instrument has previously been used to observe the organization of both an ordered and a disordered molecular monolayer on the surface,<sup>2,3</sup> and the internal structure of small adsorbed molecules.<sup>4-6</sup> For a series of related molecules on Pt(111), including naphthalene, its isomer azulene, and various methylazulenes, the details of the observed shapes permitted the identification of different isomers in mixed overlayers on the surface.<sup>7</sup> Such details can also now be predicted by a relatively simple extended Hückel molecular orbital calculation for the molecule adsorbed on a cluster of Pt atoms.<sup>7</sup> In this article, we show how STM images of the same series of molecules can be used to infer other useful molecular adsorption parameters on the Pt(111) surface, such as sticking coefficients, molecular diffusion rates, molecular orientation with respect to the substrate, and molecular binding site. Both typical low resolution images, in which different types of molecules are distinguishable, and several higher resolution images, in which internal structure of the molecules can be discerned, are shown and compared. Figure 1 shows space filling models of the seven molecules discussed in this article. The list of molecules comprises naphthalene, azulene, 1-methylazulene (1-MA), 2-methylazulene (2-MA), 6-methylazulene (6-MA), 4,8-dimethylazulene (DMA), and 4,6,8-trimethylazulene (TMA).

## II. EXPERIMENT

The multichamber ultrahigh vacuum STM apparatus with base pressure  $<10^{-10}$  Torr has been previously described elsewhere.<sup>8</sup> The Pt(111) crystal was cleaned by cycles of Ar-ion bombardment (500 eV) and flash annealing to between 800 and 900 °C. The sample was generally cooled for 45 min to 1 h to allow the sample to equilibrate at room

temperature. Molecules were dosed through a leak valve from a gas manifold heated to maintain the molecular vapor pressure near 1 Torr. Azulene and naphthalene from Aldrich and methylazulene (60% 1-MA and 30% 2-MA) from Sigma were used as received, after degassing by alternately freezing and melting under vacuum. 6-MA, DMA, and TMA were synthesized as described in Refs. 9, 10, and 11, respectively, and then deposited onto the crystal from vapor in the same manner as the other molecules. Mixed monolayers were prepared either by sequential dosing or by dosing from a mixture of bulk materials. Further details of sample preparation are given elsewhere.<sup>2,6</sup> The constant current STM measurements were mostly performed with positive sample bias, ranging from 0.05 to 1.5 V, with tunneling currents of 0.5–4 nA, and with typical image acquisition times of 5–10 min. Low and high resolution molecular corrugations were approximately 1 and 2 Å, respectively. Image processing usually consisted solely of background plane subtraction, except when explicitly stated otherwise.

## III. RESULTS AND DISCUSSION

The molecules studied in this work are very closely related, with two pairs of isomers among the seven molecules. Yet it is notable that they all have distinctive shapes when adsorbed on Pt(111), allowing the molecules to be identified on the surface even in mixed monolayers. These shapes will be described in more detail below. The discussions of the individual molecules will emphasize the differences between high and low resolution imaging, including discussion of the azimuthal orientations and binding sites. Then we will discuss in detail how STM images can be used to make inferences about adsorption parameters such as sticking coefficients and relative diffusion rates for the different molecules.

### A. Low and high resolution naphthalene

The adsorption of naphthalene on Pt(111) has been previously studied by low energy electron diffraction (LEED) and thermal desorption spectroscopy,<sup>12</sup> as well as STM.<sup>2,3,6,13</sup> The molecular organization of the ordered (6×3) overlayer of naphthalene on Pt(111), which forms at ~150 °C, has previously been discussed in detail, including the determination

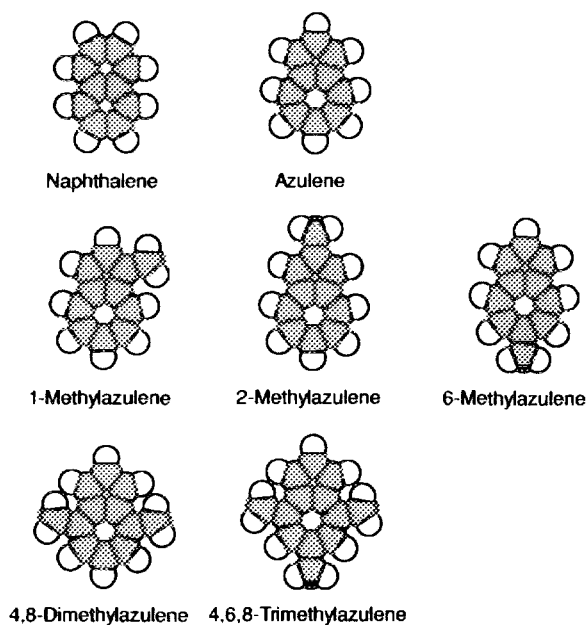


FIG. 1. Space-filling models showing structure of related molecules discussed in this article. The molecules are all shown to scale, and the van der Waals length of the naphthalene molecule is 8.1 Å.

of the azimuthal orientation with the molecular axis aligned with the Pt(111) close-packed rows and the molecular binding site on the surface being an atop site.<sup>2</sup> The structure of naphthalene overlayers has also been contrasted previously with that of its isomer azulene.<sup>6,13</sup> Therefore, we will confine the following discussion to differences between high and low resolution imaging of the molecule.

Most commonly, naphthalene appears in STM images as a double-lobed structure without other distinguishing features. Such molecular resolution is relatively easy to achieve given some persistence in obtaining a good tunneling tip. Images of this sort have been published previously and are shown later in this article in discussions of naphthalene coadsorbed with other aromatic molecules.

A high resolution image of submonolayer coverage naphthalene, on the other hand, is able to resolve both rings in the naphthalene molecule [Fig. 2(a)], as is evident when the image is statistically differenced to enhance the contrast [Fig. 2(b)]. Note that the three molecular azimuthal orientations are clearly evident, although this image has not been corrected for thermal or piezoelectric drifts. Such high resolution images can only be obtained with particular tunneling tips, which have occurred perhaps 10% of the times when we have resolved the molecules, out of many tens of experiments on this molecule. Unfortunately, we are unable to characterize our tunneling tips and therefore cannot determine whether it is the particular type or configuration of atoms at the end of the tip which makes such high resolution possible. It is clear, however, that specific tunneling voltage and current conditions are not sufficient to guarantee such extremely high resolution molecular imaging.

In some images where the naphthalene double-ring structure is resolved, it has also been possible to atomically resolve carbon atoms on the surface, as shown in the lower left

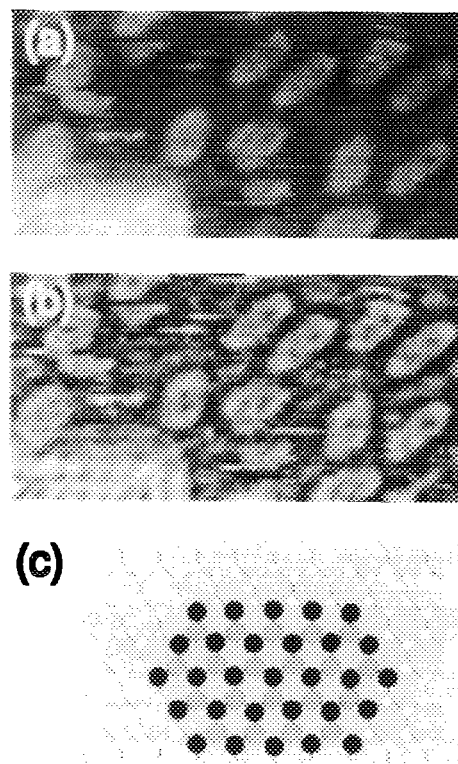


FIG. 2. High resolution STM image of naphthalene on Pt(111). (a) Top view gray scale image. (b) Statistically differenced image. (c) Sketch showing possible arrangement of graphite atoms on Pt(111). Black (gray) circles represent carbon atoms with ABC (ABA) type stacking.

corner of Figs. 2(a) and 2(b). A possible unit cell which is consistent with the data and also approximately commensurate with that of Pt(111) is shown in the sketch in Fig. 2(c). This model implies that the STM is resolving every other atom in the unit cell. In this model, all carbon sites are equivalent if only the first Pt layer is considered, so the second layer of Pt atoms must be responsible for electronic effects which result in the observed images. Note that this is similar to clean graphite, in which only the top layer atoms which do not have a neighboring atom in the second layer are observed as a result of electronic imaging effects.<sup>14</sup> Carbon superstructures like moiré patterns have been also observed when the carbon was produced from decomposition of ethylene on Pt(111).<sup>15</sup> We have not observed such structures, perhaps because the carbon islands here are formed mostly from residual carbon which did not go into the bulk upon high temperature annealing.<sup>16</sup>

## B. Monomethylazulenes

From the physical structures, 1-MA and 2-MA should be roughly kidney-bean and pear-shaped, respectively (Fig. 1). The adsorbate electronic structures expected in STM images have been computationally confirmed to be the same.<sup>7</sup> However, imaging a mixture of 1-MA and 2-MA adsorbed at low coverage on Pt(111) is difficult, since many molecules appear to be moving during the imaging (Fig. 3). Comparison of two images measured 10 min apart [Figs. 3(a) and 3(b)]

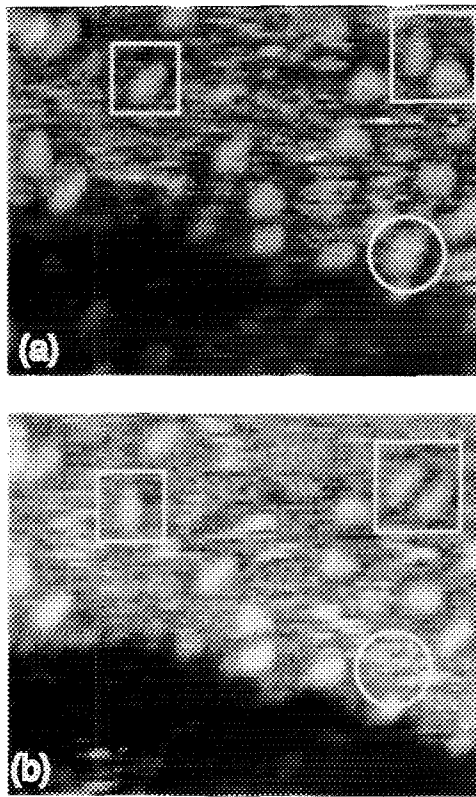


FIG. 3. Relative motion of low coverage 1-methylazulene (1-MA) (kidney-bean shapes in circles, e.g.) and 2-MA (pear-shapes in squares, e.g.) on Pt(111) between two images (a) and (b) taken 10 min apart. Note rotation of both 2-MA molecules in upper right square to be parallel in (b). Rotation of 2-MA in upper left by  $30^\circ$  is observed. 1-MA molecule in circle in (a) has moved out of local area.

indicates rotation of several 2-MA molecules as indicated. For example, in the upper right, two 2-MA molecules which are originally oriented at  $120^\circ$  (N.B., as image has not been corrected for drift, angle appears to be  $\sim 100^\circ$ ) each rotate by  $60^\circ$  to be parallel to one another. Note that many molecules are not resolved well in these images, presumably because of molecular translational motion. In particular, very few localized 1-MA molecules can be identified in Fig. 3, implying that the diffusion rate for 1-MA is higher than that for 2-MA.

When the same sample is saturated with naphthalene, the naphthalene bonds in a more highly localized way to the surface and impedes the motion of the monomethylazulene molecules, so that all three types of molecules can be clearly imaged [Fig. 4(a)]. In fact, the resulting coverage on the surface is  $\sim 50\%$  naphthalene and  $\sim 50\%$  monomethylazulenes. The 1-MA and 2-MA isomers are now clearly distinguishable in this low resolution image with more 1-MA isomers evident than in Fig. 3, now that their translational motion is hindered.

The three different monomethylazulene isomers, 1-MA, 2-MA, and 6-MA, are all readily distinguishable on Pt(111) from their observed shapes in both low and high resolution STM images. In low resolution images, 6-MA has a diamond shape [Fig. 4(b)]. This structure is again consistent with calculations for STM images of the adsorbed isomer. Interest-

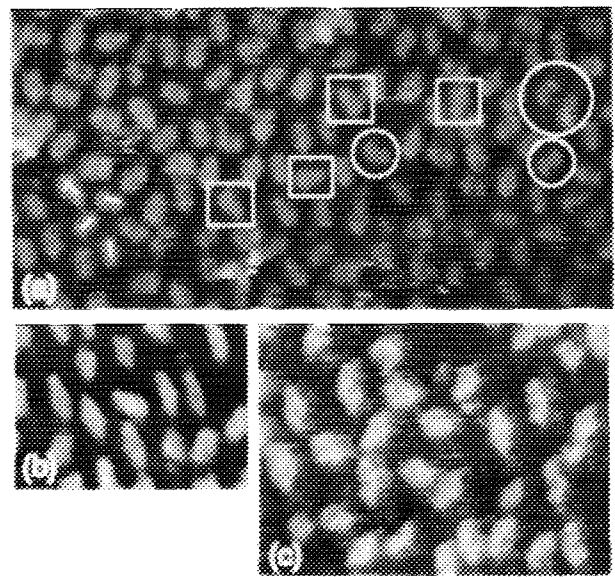


FIG. 4. (a) Same sample of 1-MA (in circles, e.g.) and 2-MA (in squares, e.g.) on Pt(111), as in Fig. 3, now saturated with naphthalene. Long bars in left corner show the three possible orientations of naphthalene molecules. The long axis of the pear-shaped 2-MA molecule, indicated by cross, is therefore oriented  $30^\circ$  from the naphthalene axis. (b) Low resolution image of 6-MA molecules, showing diamond shapes. (c) High resolution image of 6-MA, showing internal molecular structure.

ingly, the molecular orbitals for the isolated isomers appear very similar to one another, incorrectly suggesting that the methyl groups should not contribute strongly to the observed shapes of the molecules. Calculations for each type of molecule on a cluster of Pt(111) atoms, however, indicate that the distinguishing differences in shape of the electronic orbitals near the Fermi energy result from hybridization of the molecular orbitals with those of the metal substrate, resulting in contributions to the density of states near the positions of the methyl groups.<sup>7</sup>

The three possible azimuthal orientations of naphthalene on Pt(111) are marked on several molecules in the lower left corner of Fig. 4(a). By comparing the orientation of a 2-MA molecule with those of neighboring naphthalenes, it is clear that the axis of the 2-MA is inclined by  $30^\circ$  with respect to that of naphthalene, and therefore also with respect to the close-packed rows of the Pt lattice. Unfortunately, for 1-MA, the resolution of the image does not permit an assignment of the molecular axis. Three possible azimuthal orientations of 6-MA, however, are easily observed in Fig. 4(c); in addition the two possible directions of the molecule along each azimuth are also observed.

### C. Trimethylazulene (TMA)

TMA appears in most of the STM images as a fourfold cloverleaf structure (Fig. 5). Many molecules appear with a bright spot on one lobe. The physically reasonable assignment, based on symmetry of the molecule, that the bright spot corresponds to the position of the five-membered ring is confirmed by extended Hückel calculations.<sup>7</sup> When TMA is coadsorbed with naphthalene, we see that the axis through

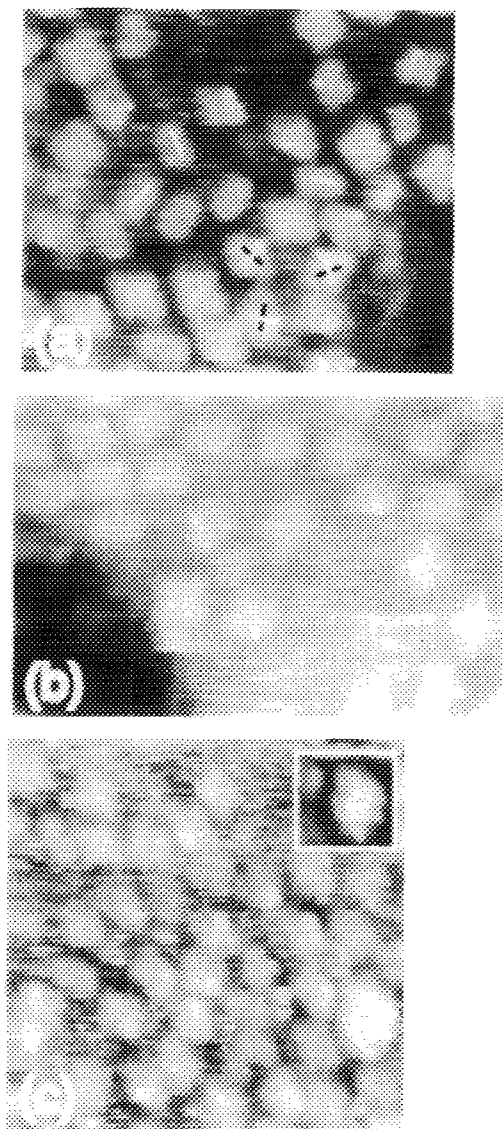


Fig. 5. Trimethylazulene on Pt(111). (a) Well-resolved image showing relative orientations of trimethylazulene (indicated by cross, with white bar indicating axis of molecule through rings) with respect to neighboring naphthalene molecules (indicated by white bars). (b) High resolution image showing a bright spot on many trimethylazulene molecules, with some translational diffusion of molecules evident. (c) Well-resolved image of trimethylazulene molecules with high resolution image of second layer molecule from lower right shown with enhanced contrast in inset; hole in center of molecule is evident in enhanced image.

the rings of the TMA molecule is aligned with that of a neighboring naphthalene molecule [Fig. 5(a)], and therefore also with the close-packed rows of the Pt(111) lattice. All three possible azimuthal orientations of the TMA axis are observed. The same symmetry arguments used to assign naphthalene to an atop site, namely the requirement for a sixfold site, are applicable to TMA. The observed ( $4 \times 4$ ) LEED pattern is consistent with the larger molecular size of TMA relative to naphthalene [which packs in ( $3 \times 3$ ) arrays] and agrees well with the molecular spacings measured in these STM images.

Most TMA molecules are clearly resolved as fourfold structures in Fig. 5(b), with a bright spot observable on many

of them. The absence of a bright spot on some molecules could be explained by molecular motion during an image. The preservation of the cloverleaf-shape rules out  $120^\circ$  rotations of the molecule, but  $180^\circ$  flips are consistent with this shape. Molecular rotation during STM imaging has previously been observed for naphthalene when the molecule appears to rotate about one lobe.<sup>6</sup> Some areas on the surface have the horizontal scan line features which are characteristic of translational molecular diffusion.<sup>6</sup>

In Fig. 5(c), again most TMA molecules are well resolved. One very bright molecule is observed in the lower right hand corner of the image and shown with increased contrast in the inset. This molecule may be in the second layer and thus appear taller. It appears to have a hole in the center. More molecules displaying such holes in the center are shown in Fig. 6(a), an image measured at lower coverage with widely separated molecules and a tip with infrequently attained high resolution.

In some cases, even with degraded imaging caused by a double tip, one can still clearly identify TMA molecules [Fig. 6(b)]. Here the molecules still retain their distinctive fourfold shapes. Note that they show no particular tendency to clump near the atomic step in the lower part of the image.

#### D. Dimethylazulene (DMA)

DMA has a shape very similar to that of TMA in STM images [cf. Figs. 5, 6(a), and 6(b)]. Apparently, the methyl group in the 6 position for TMA does not contribute strongly to the observed electronic density of states, resulting in the observed images for DMA and TMA looking so similar. The similar shapes of the STM images for these molecules can also be predicted from our theoretical calculations of the electronic density of states.<sup>7</sup>

Figure 6(c) shows very graphically the differing resolutions obtained when a sudden tip change occurred as the tip passed over a particularly high defect on the surface. The first part of the image (bottom) had very high resolution, showing the four lobes of the molecule with one bright feature, while the second part of the image (top) after the tip change shows severely degraded resolution so that one observes only amorphous shapes for the molecules.

#### E. Sticking coefficients and diffusion rates

Naphthalene is clearly a very stable molecule which is strongly chemisorbed on Pt(111) with a relatively high sticking coefficient. A dosage of  $\sim 0.1$  langmuir (L), uncorrected for gauge sensitivity, leads to saturation coverage of  $\sim 1$  monolayer (ML) of naphthalene. Naphthalene packs in a ( $3 \times 3$ ) structure on Pt(111), giving one naphthalene molecule per nine metal atoms, which is consistent with the sticking coefficient of nearly unity. Molecular motion is not observed at room temperature (RT) within the ordered overlayer which forms only at slightly elevated temperatures. For 0.2 ML coverage or at the domain boundaries in ordered overlayers, occasional molecular rotations and translations at RT have been observed on comparing consecutive images  $\sim 10$  min apart.<sup>2,3</sup>

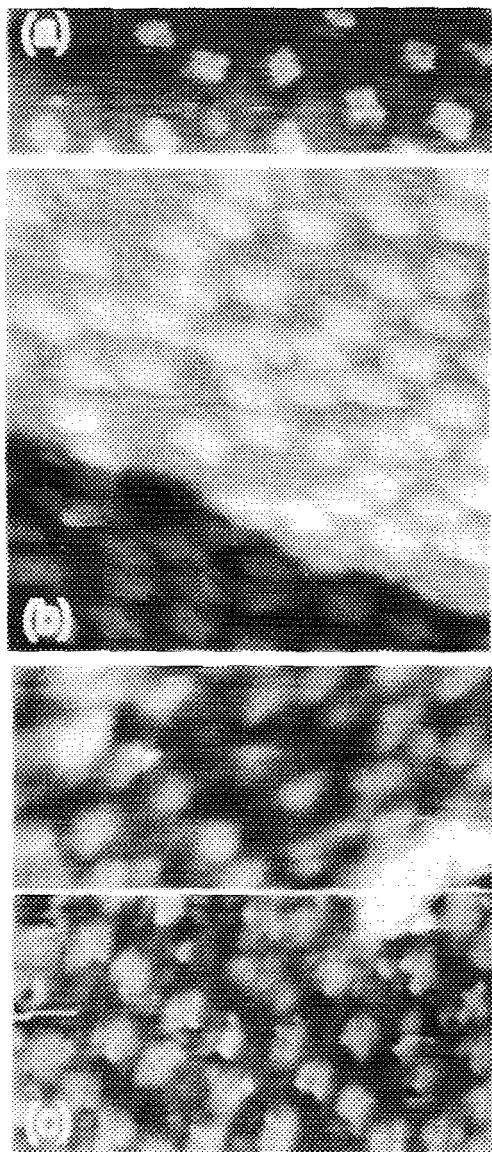


FIG. 6. (a) Low coverage of trimethylazulene on Pt(111), with molecules appearing more like squares, with small holes in centers. (b) Trimethylazulene molecules resolved well as clover leaf structures, despite imaging by double tip. (c) Dimethylazulene molecules on Pt(111), with high resolution imaging at bottom degrading severely after tip hit high spot on surface, resulting in much lower resolution in top half of image.

In contrast, its isomer azulene is much more difficult to resolve clearly with the STM. Low coverage measurements resolve very few molecules because of high translational diffusion rates. This results in the molecules moving rapidly during the image acquisition time of our instrument, so that individual molecules are observed easily in a single scan line but are not stable enough to form a consistent image over several scan lines. Comparisons of saturation dose requirements reveal the sticking coefficient of azulene to be about  $\frac{1}{4}$  that of naphthalene. Finally, even in an ordered ( $3 \times 3$ ) monolayer, low resolution images show only circular molecules with no distinguishing features. High resolution images appear to resolve a single ring.<sup>6,13</sup> We have speculated previously that rotational motion could explain why the im-

ages look round, rather than showing submolecular detail which was predicted in our extended Hückel molecular orbital calculations for a single molecule on a cluster of Pt atoms.<sup>7</sup>

The monomethylazulene isomers, 1-MA and 2-MA, appear to have diffusion rates intermediate between those of naphthalene and azulene. Very few 1-MA isomers are identified at low coverage compared with the same sample saturated with naphthalene, while more 2-MA isomers are observed at both coverages [Figs. 3 and 4(a)]. Thus, 1-MA seems to have a higher diffusion rate than 2-MA. On the other hand, 6-MA seems to diffuse less than the other monomethylazulenes and is thus more easily imaged by the STM.

The sticking coefficients of the molecules studied here can also be inferred by comparing their relative exposures with their resulting coverages in STM images. In this way, we had previously determined the relative sticking coefficients  $\sigma_{\text{naphthalene}}/\sigma_{\text{azulene}} \approx 4$  and  $\sigma_{1\text{-MA}}/\sigma_{2\text{-MA}} \approx 0.2$ .<sup>6</sup> The coverage of 2-MA when coadsorbed with naphthalene in Fig. 4(a) is approximately 50%, as discussed earlier, when dosed sequentially with identical exposures of  $\sim 0.1$  L. This same exposure is known to yield approximately 1 ML of naphthalene on the surface, implying that  $\sigma_{\text{naphthalene}}/\sigma_{2\text{-MA}} \approx 2$ . An estimate of surface coverage for TMA from STM images, using  $4 \times 4$  packing on the Pt lattice to give area/molecule, yields  $\sim 50\%$  coverage for an exposure of  $\sim 0.3$  L, giving the ratio of sticking coefficients  $\sigma_{\text{naphthalene}}/\sigma_{\text{TMA}} \approx 6$ .

#### IV. CONCLUSIONS

We have compared the STM images of a series of related molecules. Each molecule in the series can be identified by its shape in a good low resolution STM image. In higher resolution images, details of the internal molecular structure become evident. Such details have previously been shown to agree well with calculations.<sup>7</sup> Coadsorbed molecular layers are particularly useful because they eliminate tunneling tip effects when comparing different types of molecules in the same image, and also enable the direct comparison of the images of the coadsorbed molecules. The relative azimuthal orientations of the molecules can usually be obtained by inspection from such images. Binding sites for molecules can sometimes be obtained by comparing with previously determined sites for other molecules. Finally, molecular diffusion rates and sticking coefficients can be inferred by comparing molecular exposure during deposition with coverage measured directly from the STM images. Species with low diffusion rates, such as naphthalene and 6-MA, are more readily imaged with high resolution. Thus, with care, STM images can be used not only to identify molecules on the surface, but also to determine many molecular adsorption parameters.

#### ACKNOWLEDGMENTS

The authors would like to acknowledge helpful discussions with T. A. Land and M. Salmeron.

<sup>1</sup>S. Chiang, in *Scanning Tunneling Microscopy I*, edited by H.-J. Guntherodt and R. Wiesendanger (Springer, Berlin, 1992), pp. 181–205.

- <sup>2</sup>V. M. Hallmark, S. Chiang, J. K. Brown, and Ch. Woell, *Phys. Rev. Lett.* **66**, 48 (1991).
- <sup>3</sup>V. M. Hallmark, S. Chiang, and Ch. Woell, *J. Vac. Sci. Technol. B* **9**, 1111 (1991).
- <sup>4</sup>H. Ohtani, R. J. Wilson, S. Chiang, and C. M. Mate, *Phys. Rev. Lett.* **60**, 2398 (1988).
- <sup>5</sup>P. H. Lippel, R. J. Wilson, M. D. Miller, Ch. Woell, and S. Chiang, *Phys. Rev. Lett.* **62**, 171 (1989).
- <sup>6</sup>V. M. Hallmark and S. Chiang, *Surf. Sci.* **286**, 190 (1993).
- <sup>7</sup>V. M. Hallmark, S. Chiang, K.-P. Meinhardt, and K. Hafner, *Phys. Rev. Lett.* **70**, 3740 (1993).
- <sup>8</sup>S. Chiang, R. J. Wilson, Ch. Gerber, and V. M. Hallmark, *J. Vac. Sci. Technol. A* **6**, 386, (1988).
- <sup>9</sup>K. Hafner and K.-D. Asmus, *Liebigs Ann. Chem.* **671**, 31 (1964).
- <sup>10</sup>K. Hafner and H. Weldes, *Liebigs Ann. Chem.* **606**, 90 (1957).
- <sup>11</sup>K. Hafner and H. Kaiser, *Liebigs Ann. Chem.* **618**, 140 (1958); *Org. Synth. Coll.* **5**, 1088 (1964).
- <sup>12</sup>D. Dahlgren and J. C. Hemminger, *Surf. Sci.* **109**, L513 (1981); **114**, 459 (1982), and references therein.
- <sup>13</sup>V. M. Hallmark, S. Chiang, J. K. Brown, and Ch. Woell, in *Synthetic Microstructures in Biological Research*, edited by J. M. Schnur and M. Peckerar (Plenum, New York, 1992), pp. 79–90.
- <sup>14</sup>I. P. Batra, N. Garcia, H. Rohrer, H. Salemink, E. Stoll, and S. Ciraci, *Surf. Sci.* **181**, 126 (1987).
- <sup>15</sup>T. A. Land, T. Michely, R. J. Behm, J. C. Hemminger, and G. Comsa, *Appl. Phys. A* **A53**, 414 (1991); *Surf. Sci.* **264**, 261 (1992).
- <sup>16</sup>R. Vanselow and M. Mundscha, *J. Phys. C* **7**, 117 (1986); M. Mundscha and R. Vanselow, *Surf. Sci.* **160**, 23 (1985); *J. Phys. C* **7**, 121 (1986).